Neuromorphic Biophotonic Sensor Based on Near Infrared Optical Reflectometry

Jae-Ho Han, *Member, IEEE*, and Jin U. Kang, *Member, IEEE*

Abstract—A biophotonic image sensor has been demonstrated by depositing a thin Au (gold) film on the single optical fiber by sputtering process to incorporate a self-contained reference plane, as well as to be sustainable for different contact interfacial medium. This side-viewing optical probe has been polished for 43°–49° angle in order to unilaterally reflect the beam to be focused with a micro dome-shape lens simply formed by high-energy melting process at the distal end of the standard single-mode fiber. The all fiber interferometric optics using a low (partial) coherence double-sided autocorrelator performing as a high-precision optical reflectometer at 1300 nm range noninvasively conducted a direct profiling of the depth information inside a biological tissue and for diagnosing brain tumors, as well as imaging subsurface depth profile for other turbid organic/inorganic samples. The optical probing imager, which normally operates in low power of 3 mW–7 mW has ∼35 dB signal-to-noise ratio (SNR) and a ∼15 μm axial resolution (3-dB width of the reflected peak curve).

Index Terms—Biomedical measurements, biomedical transducers, image sensors, optical fiber devices, optical reflectometry.

I. INTRODUCTION

HIGH-resolution cross-sectional noninvasive and real-time optical imaging has been used to measure depth-resolved images to differentiate between the cancer and normal tissues in esophagus, colon, and coronary [1], [2]. Particularly, for neuromorphic (structural) and functional imaging and image-guided surgery, there have also been great efforts to early diagnose various kinds of tumors and cancers such as glioma and melanoma, as well as detecting the vein in which information directly inside the tissue if is necessary [3], [4]. However, there is only limited space within biological object so that most of conventional scanning probes are limited for their endo/microscopic *in vivo* imaging of internal micro tissues [5]–[7]. Thus, to meet the above mentioned concerns for a specific circumferential visualization, various kinds of side-viewing micro-optic probes have been suggested in a

variety of sensing and imaging modalities [8]–[14]. Especially, in the previous report in [15], feasibility of the bare-fiber side-viewing probe was demonstrated with inserting a separate external microlens that can focus the output beam to have a better lateral resolution than that of normal diverging bare fiber-optic probes without beam concentration. Furthermore, it has failed to achieve an appropriate strong level of self-contained interferometric reference that can practically work due to the small reflectance at the polished fiber interface so that an external partial reflector has been employed instead to accomplish that purpose only for free-space standing specimens (it usually requires a air gap between the imaging probe and the sample for having a reference signal). Those external bulk optic components eventually make the probing imaging sensor to be greater in overall size, as well as embrace alignment issues in between. In this work, a true integrated micro side-viewing fiber-optic probe (∼125 μm) has been fabricated that can be inserted directly into the brain for profiling depth images coated with a semitransparent thin gold (Au) film that allows a self-incorporated reference plane, an essential part for optical reflectometry-based interferometric imaging, from the distal end of the probe without using additional external semitransparent and/or partial reflectors for achieving references or other bulk optics. This technique, in principle, is similar to the conventional electrical or optical time-domain reflectometry (TDR, OTDR), where it localizes and determines the discontinuity or faults from the reflected waveforms for the specimen with a finer dead zone or resolution by using the mixing interference of a broadband light source. Additionally, gold coating which is a biomedically safe material provides and optical protection by avoiding the effect of refractive index dependence of an interfacial contact medium on the reference amplitude whether the probe works in a free-space standing or aqueous environment, even in contact with the specimen. Moreover, in order to achieve beam focusing, a micro dome-shape lens has been fabricated which enables a simple integration without adapting external focusing elements by a high-energy melting process. The angle polished fiber aims the beam for circumferential view by strong interface internal reflection on the gold-coated layer in which one-way directional beam is suitable for the integration with conventional medical hypodermic needles having asymmetrical shapes where one side can be considered as an optical biopsy window. The fiber-optic probe has been characterized as well as its signal-to-noise ratio (SNR) performance and its ability for depth imaging for various specimens including a brain sample of a rat for the potential usage in noninvasive optical biopsy and diagnosis as well as cross-sectional subsurface image profiler.

J.-H. Han was with the Department of Electrical an d Computer Engineering, Johns Hopkins University, Baltimore, MD 21218 USA. He is now with the Department of Brain and Cognitive Engineering, Korea University, Seoul, 136-713 South Korea (e-mail: jhhan16@gmail.com).

J. U. Kang is with the Department of Electrical and Computer Engineering, Johns Hopkins University, Baltimore, MD 21218 USA (e-mail: jkang@jhu.edu).
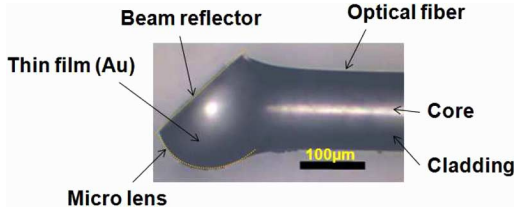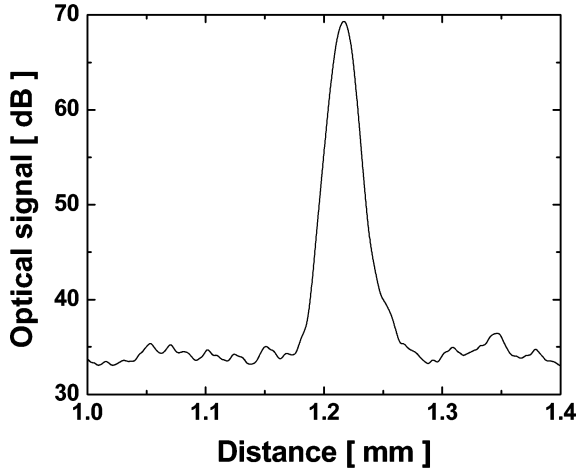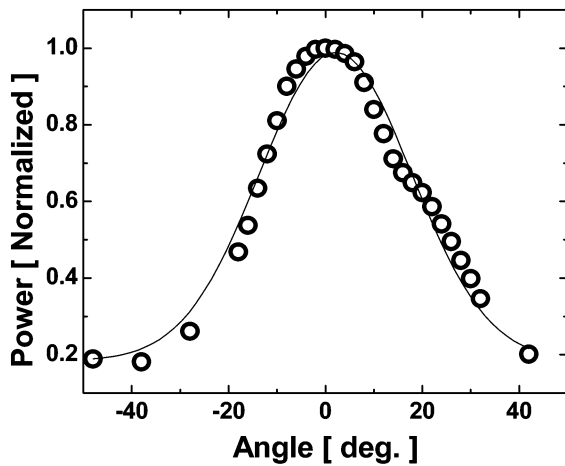
Fig. 1. Example photo of the fabricated thin-film gold-coated side-viewing fiber-optic imaging microprobe and its layout.

(a)

(b)

Fig. 2. Characteristics of side-viewing microprobes. (a) Reference coherence autocorrelated amplitude signal. (b) Beam far-field profile (circle: measured result, solid line: curve fitting).

Fig. 3. SNR versus output power: circle-measured, solid line-fitted trend curve.

(a)

$$E_{tot}(t) = E_r(t) + E_s(t + \tau_s)$$

(b)

Fig. 4. Experimental setup for all fiber-optical interferometric-based sensor. (a) Schematic view. (b) Push-pull fiber-based double-sided autocorrelator configuration.

II. THIN-FILM GOLD-COATED SIDE-VIEWING IMAGER

The side-viewing microprobe in the inset of Fig. 1 ($200\times$ magnification, photo taken by a digital microscope, scale bar indicates 100 μm) was fabricated from a standard single-mode optical fiber (SMF-28), where a micro-ball lens was formed either (diameter of ball size is around 200 μm) by exposing to a high-power CO_2 laser or by melting with using a commercial arc-fusion fiber splicer. It was angled ($43°$–$49°$) by polishing in one side for internal beam reflection so that the remaining lens is used to focus the forward directed beam. A thin gold film was optimized for its reflection and transmission to be deposited for
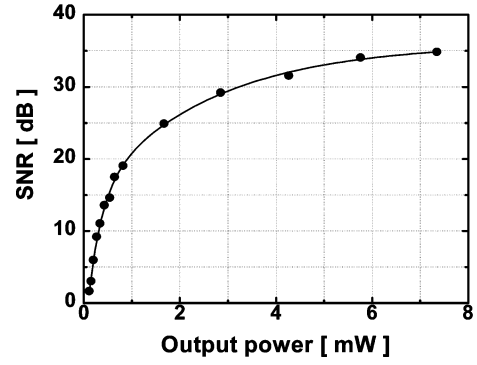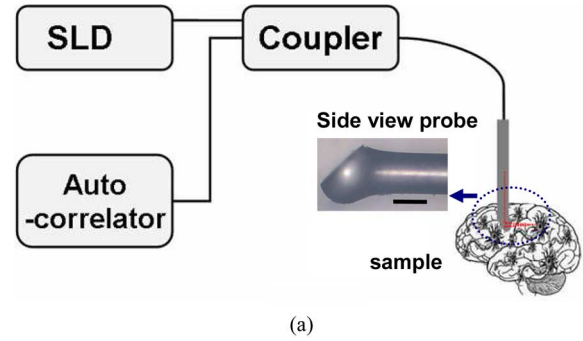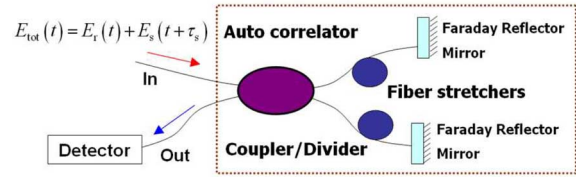
approximately 20 s using a conventional semiconductor sputtering process (Denton Vacuum DESK II) with a gold-palladium (Au-Pd) alloy on the end face of the fiber tip in order to fabricate a uniform metallic layer [16].

The gold-coated probe was characterized by measuring the reference coherence peak signal (or the point spread function of the probe) from the probe tip, as shown in Fig. 2(a), having a symmetrical peak of $\sim$35 dB amplitude above noise background. The measured A-scan (depth) resolution or the -3 dB width of the reference peak of 15 μm was determined by the coherence length of the low-coherence light source. At this point, we should mention that, without the gold coating, it was rather hard not only to couple back certain level of reference amplitude [coherence peak as in Fig. 2(a)] from the bare fiber probe with the same structure due to the fractional reflectance from the distal end of the fiber between the glass-air interface, as well as its structural dimension so that additionally, instead, an external bulk partial reflector would preferably be inserted for stronger reference signal [15], accordingly, but also to reconstruct the returned sample signal for sensing. In this case without gold-coating, even if there exists a small amount of reference amplitude in a free-space, once the probe is in contact with a
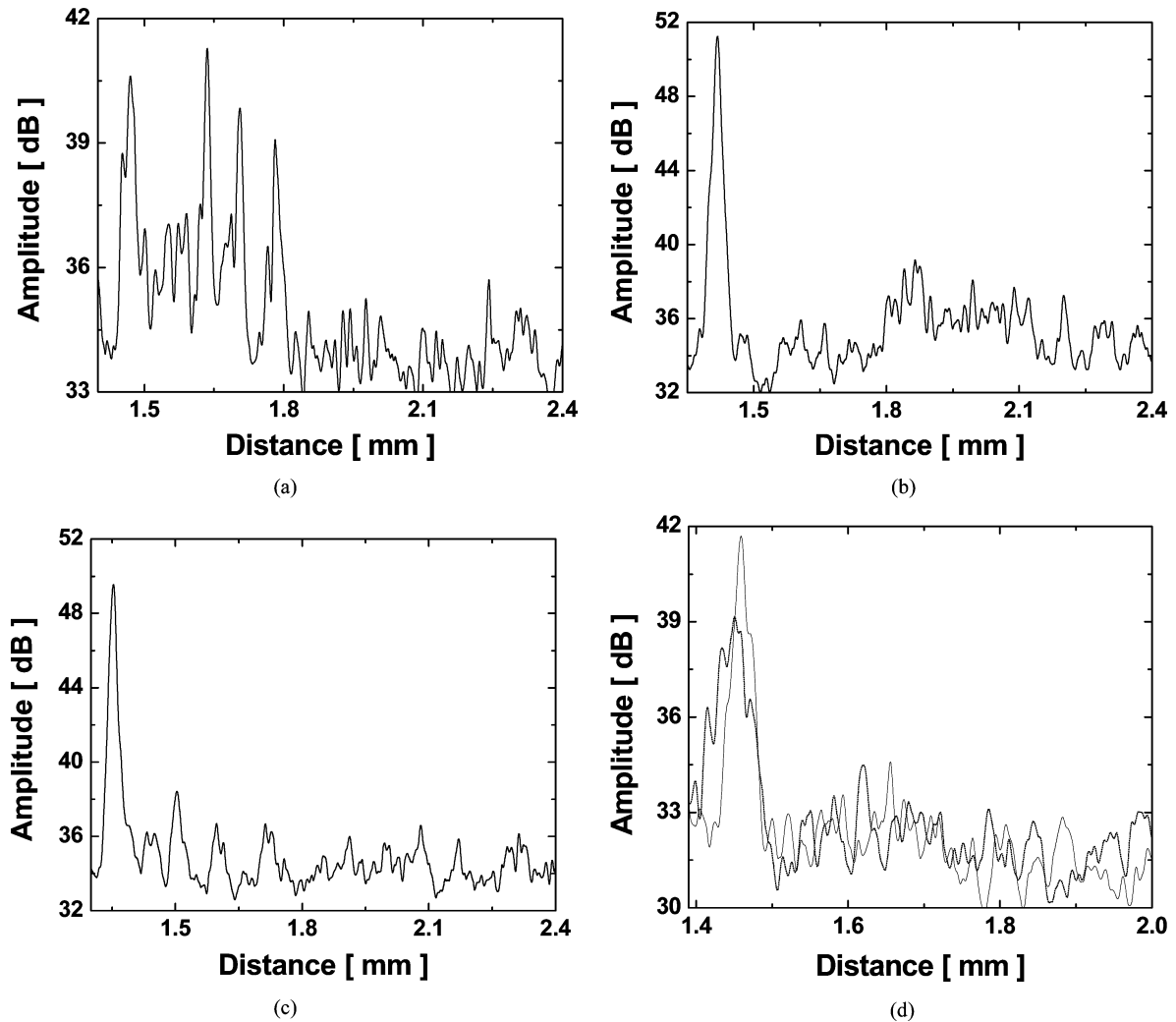
Fig. 5.   Captured image using a gold-coated side-viewing fiber tip: (a) polymer tape layers; (b) IR sensing card (single polymer layer + organic material); (c) onion skin; (d) Rat brain (solid line: normal, dotted line: tumor).

specimen or put in an aqueous condition the reference magnitude significantly drops by the reduced refractive index difference between the glass fiber and the contact medium. Here, the reference level of the gold-coated probe depends not only on the thickness of the gold coating but on the dimension of the microlens to have enough distance for diverging before making a focus, where the Rayleigh distance is approximately 70 μm [16]. The far-field pattern of the beam is measured (circle) depending on the angles in Fig. 2(b), where the full width at half maximum (FWHM) is around $43°$ and the beam has a Gaussian line shape (solid line). The SNR of the probing system is measured to be stable around 30–35 dB throughout the normal operating power range of 3–7 mW. The result is shown in Fig. 3 where the solid circle and the line curve are the measured and fitted trend curve results, respectively. Although this SNR result is relatively lower than conventional forward viewing CPOCT by 10–15 dB [17] due to the signal attenuation that can occur possibly in the metallic layer, it is still comparable with the SNR reported in [15] having SNR of 35 dB. However, only limited reports have already provided SNR (7–11 dB) [8] or minimum sensitivity (130 dB, 80 dB) [10], [12] for side-viewing imagers in different modalities that can be compared with the proposed

side-viewing probe. The lateral (transverse) resolution of an optical fiber-based imager is limited by its core dimension (numerical aperture of optical fiber) which is approximately 10 μm [15] or 6.8 μm [12].

III. Experiment and Results

The introduced all fiber-optical imaging system is based on a near infrared (IR) optical reflectometer, where a 1.3 μm range source of super-luminescence diode (SLD) having a Gaussian spectral shape was used as a low coherence light, as in Fig. 4(a) [17]. In the design described above, the electric field E_r is partially reflected to form a reference, while the transmitted part of the light illuminates the sample. The total electric field signal $E_{tot}(t)$ collected from the fiber probe comprises of the reference, E_r and the sample, E_s with a time delay τ_s. The optical autocorrelator extracts the depth information from the convolution between those reference and the sample signals where the time delay or path difference for determining different depths is accomplished by the piezo-electric controlled fiber stretchers and Faraday reflector mirrors, as shown in Fig. 4(b). Here, a path-balanced autocorrelator for the upper and the lower paths produces a symmetric double-sided signal, like the scan region,

e.g., from minus 4 mm to positive 4 mm in the system, with the position of the coherence peak at the center. However, introducing an offset in the two arms—the difference between the path lengths of two arms in the scanning interferometer, such as a 3 mm offset can be used to achieve desired longitudinal scan region from minus 1 mm to positive 7 mm. Hence, this autocorrelator with a correct offset in optical path lengths can mimic a typical Michelson interferometer for all practical purposes. Here, the interference pattern occurs only if the path difference lies within the coherence length of the low coherence source, which is the depth resolution of the imaging system. The photodiode (PD) detects the amplitude of each path changes to map the autocorrelation result as a function of distance. For the common optical path-based interferometer configuration, the reference signal is achieved from the partial reflection at the distal end of the fiber probe and the sample signals are from the reflections at the specimen's surface and inner substructures with different refractive indices or with tissue scattering [18]. Using 1300 nm near IR source supports longer penetration depth than that of other shorter infrared sources due to less scattering in the tissue in a rather constant attenuation by photon absorption. The behavior of photons is dominated by scattering and the individual path of a given single photon is modeled as a random walk so that a large number of photons exhibit diffusion in the medium [19]. The low coherence interferometric imaging is based on the detection of coherent photon transport in which the light photons travel through a scattering turbid medium. In this turbid medium, most of the incident photons experience a random scattering and absorption whereas, for a short distance, a few photons can diffuse in a straight path.

For internal structure sensing from the specimen, the gold-coated fiber probe was placed in close proximity to the *ex vivo* sample. Typical images for the different specimens are shown in Fig. 5. We can observe multiple-layer stacks of organic cellophane represented as peaks in Fig. 5(a); high reflection at the front polymer surface of the infrared detection card as well as the inner organic structures in Fig. 5(b); the multiple reflections were observable due to the hyper reflection of the onion skin cells or inner microstructures in Fig. 5(c); and a rat brain having parts of normal and tumor (melanoma) can be differentiated by the subsurface scattering or reflection patterns in Fig. 5(d). The normal healthy part (solid line) has a thin but strong surface reflection, whereas tumor has highly scattered features shown by broader overlapped peaks (dotted line) near the surface, which match to the previous results [17]. It is also able to observe deeper cerebral cortex layers represented by satellite peaks apart from the brain surface.

IV. CONCLUSION

The internal depth information sensing of biological tissue (onion) and diagnostic feature of brain tumor as well as other organic/inorganic (polymer layers) specimens have been successfully demonstrated using the microlens integrated side-viewing gold-coated microfiber probe based on optical autocorrelator using partial coherence reflectometer at 1.3 μm. The fabricated gold-coated microtip was able to conduct noninvasive cross-sectional imaging without external bulk reference plane and focusing lens, which are desirable features for the potential use in a variety of minimally invasive high-resolution ($\sim$15 μm) neuromorphic imaging and disease diagnostic/biopsy procedures.

REFERENCES

[1] B. E. Bouma and G. J. Tearney, "Power-efficient nonreciprocal interferometer and linear-scanning fiber-optic catheter for optical coherence tomography," *Opt. Lett.*, vol. 24, pp. 531–533, 1999.

[2] Q. Zhu, D. Piao, M. M. Sadeghi, and A. J. Sinusas, "Simultaneous optical coherence tomography imaging and beta particle detection," *Opt. Lett.*, vol. 28, pp. 1704–1706, 2003.

[3] S. W. Jeon, M. A. Shure, K. B. Baker, D. Huang, A. M. Rollins, A. Chahlavi, and A. R. Rezaia, "A feasibility study of optical coherence tomography for guiding deep brain probes," *J. Neurosci. Methods*, vol. 154, pp. 96–101, 2006.

[4] H. J. Böhringer, E. Lankenau, F. Stellmacher, E. Reusche, G. Hüttmann, and A. Giese, "Imaging of human brain tumor tissue by near-infrared laser coherence tomography," *Acta Neurochir.*, vol. 151, pp. 507–517, 2009.

[5] H. Li, B. A. Standish, A. Mariampillai, N. R. Munce, Y. Mao, S. Chiu, N. E. Marcon, B. C. Wilson, A. Vitkin, and V. X. D. Yang, "Feasibility of interstitial Doppler optical coherence tomography for in vivo detection of microvascular changes during photodynamic therapy," *Lasers Surg. Med.*, vol. 38, pp. 754–761, 2006.

[6] Y. Chen, A. D. Aquirre, L. Ruvinskaya, A. Devor, D. A. Boas, and J. G. Fujimoto, "Optical coherence tomography (OCT) reveals depth-resolved dynamics during functional brain activation," *J. Neurosci. Methods*, vol. 178, pp. 162–173, 2009.

[7] U. M. Rajagopalan, K. Tsunoda, and M. Tanifuji, "Using the light component of optical intrinsic signals to visualize in vivo functional structures of neural tissues," *Methods Mol. Biol.*, vol. 489, pp. 111–132, 2009.

[8] C. J. de Lima, S. Sathaiah, M. T. T. Pacheco, R. A. Zângaro, and R. Manoharan, "Side-viewing fiberoptic catheter for biospectroscopy applications," *Laser Med. Sci.*, vol. 19, pp. 15–20, 2004.

[9] H. Tanaka, G. Yamada, T. Saikai, M. Hashimoto, S. Tanaka, K. Suzuki, M. Fujii, H. Takahashi, and S. Abe, "Increased airway vascularity in newly diagnosed asthma using a high-magnification bronchovideoscope," *Amer. J. Respir. Cri. Care Med.*, vol. 168, pp. 1495–1499, 2003.

[10] Y. Wu, J. Xi, L. Huo, J. Padvorac, E. J. Shin, S. A. Giday, A. M. Lennon, M. I. F. Canto, J. H. Hwang, and X. Li, "Robust high-resolution fine OCT needle for side-viewing interstitial tissue imaging," *IEEE J. Sel. Top. Quant. Electron.*, vol. 16, pp. 863–869, 2010.

[11] G. Iaquinto, M. Fornasarig, M. Quaia, N. Giardullo, V. D'Onofrio, S. Iaquinto, S. Di Bella, and R. Cannizzaro, "Capsule endoscopy is useful and safe for small-bowel surveillance in familial adenomatous polyposis," *Gastrointest. Endosc.*, vol. 67, pp. 61–67, 2008.

[12] H. Y. Choi, S. Y. Ryu, J. Na, B. H. Lee, I.-B. Sohn, Y.-C. Noh, and J. Lee, "Single-body lensed photonic crystal fibers as side-viewing probes for optical imaging systems," *Opt. Lett.*, vol. 33, pp. 34–36, 2008.

[13] E. Frimberger1, S. von Delius, T. Rösch, and R. M. Schmid, "Colonoscopy and polypectomy with a side-viewing endoscope," *Endoscopy*, vol. 39, pp. 462–465, 2007.

[14] D. S. Elson, J. A. Jo, and L. Marcu, "Miniaturized side-viewing imaging probe for fluorescence lifetime imaging (FLIM): Validation with fluorescence dyes, tissue structural proteins and tissue specimens," *New J. Phys.*, vol. 9, p. 127, 2007.

[15] U. Sharma and J. U. Kang, "Common-path optical coherence tomography with side-viewing bare fiber probe for endoscopic optical coherence tomography," *Rev. Sci. Instrum.*, vol. 78, p. 113102, 2007.

[16] J.-H. Han, I. K. Ilev, D.-H. Kim, C. G. Song, and J. U. Kang, "Investigation of gold-coated bare fiber probe for in situ intra-vitreous coherence domain optical imaging and sensing," *Appl. Phys. B*, vol. 99, pp. 741–746, 2010.

[17] X. Li, J.-H. Han, X. Liu, and J. U. Kang, "Signal-to-noise ration analysis of all-fiber common-path optical coherence tomography," *Appl. Opt.*, vol. 47, pp. 4833–4840, 2008.

[18] K. M. Tan, M. Mazilu, T. H. Chow, W. M. Lee, K. Taguchi, B. K. Ng, W. Sibbett, C. S. Herrington, C. T. A. Brown, and K. Dholakia, "Infiber common-path optical coherence tomography using a conical-tip fiber," *Opt. Express*, vol. 17, pp. 2375–2384, 2009.

[19] K. M. Yoo and R. R. Alfano, "Time-resolved coherent and incoherent components of forward light scattering in random media," *Opt. Lett.*, vol. 15, pp. 320–322, 1990.

Jae-Ho Han (M'03) received the B.S. and M.S. degrees in electronic engineering and radio engineering from Korea University, Seoul, Korea, in 1998 and 2000, respectively, and Ph.D. degree in electrical and computer engineering from Johns Hopkins University, Baltimore, MD, in 2010.

Since 2010, he has been with the Physical Measurement Laboratory (PML), National Institute of Standards and Technology (NIST), Gaithersburg, MD, as a Postdoctoral Associate. From 2000 to 2005, he was an Associate Researcher at the Fiber Optics and Telecommunication Laboratory, LG R&D Center, Anyang, where he was engaged in the research and development of high-speed optoelectronic devices and optical transmission systems. His current research interests include interface state spectroscopy, near infrared lasers, and their application to biomedical sensor and imaging technology.

Jin U. Kang (M'00) received the Ph.D. degree in electrical engineering and optical sciences from the University of Central Florida, Orlando, in 1996.

From 1996 to 1998, he was a Research Engineer with the United States Naval Research Laboratory, Washington, DC. He is currently a Professor and Chair in the Department of Electrical and Computer Engineering, Johns Hopkins University, Baltimore, MD. His research interests include fiber-optic sensors and imaging systems, novel fiber laser systems, and biophotonics.